International Symposium
On Turbulence and Shear Flow
Phenomena (TSFP-8)
August 28 - 30, 2013 Poitiers, France

PARTICLE-TURBULENCE INTERACTIONS IN THE PRESENCE OF A ROUGH WALL

Godwin F.K. Tay
Department of Mechanical and Manufacturing Engineering
University of Manitoba
Winnipeg, MB, Canada R3T 5V6
umtayg@cc.umanitoba.ca

David C.S. Kuhn
Department of Mechanical and Manufacturing Engineering
University of Manitoba
Winnipeg, MB, Canada R3T 5V6
dkuhn@cc.umanitoba.ca

Mark F. Tachie
Department of Mechanical and Manufacturing Engineering
University of Manitoba
Winnipeg, MB, Canada R3T 5V6
tachiemf@cc.umanitoba.ca

ABSTRACT

Experiments were conducted over smooth and rough walls in a low Reynolds number horizontal turbulent channel flow laden with small (64 μm) glass particles. A particle image velocimetry technique was used to measure velocities of both the carrier fluid and particles. Various turbulent characteristics were examined to investigate the impact of wall roughness on the particle-turbulence interactions. The results show that particles increased the turbulent intensities near the wall, and reduced them in the outer layer, but these effects were dampened for the rough wall. On the contrary, particles increased the peak value of the Reynolds shear stress in the presence of the rough wall when compared to the unladen flow. Particle velocity fluctuation intensities matched those of the unladen fluid for the smooth wall, but the peak velocity fluctuation intensities were enhanced in the presence of wall roughness due to particle-wall collisions. The effect is larger for the streamwise velocity fluctuation intensity than the wall-normal velocity fluctuation intensity. The present results indicate that the particle motion is more responsive to the presence of the rough wall than the particle-laden fluid.

INTRODUCTION

Turbulent flows laden with particles are common in many engineering applications. Examples include fluidized beds, pneumatic conveying and pollution control systems. Understanding these flows as well as developing their model representations demands knowledge of the interaction between particles and fluid turbulence. It has been suggested that depending on the size, density ratio and particulate phase loading, the interaction may lead to modification of the fluid turbulence level. The type of interaction between the particles and fluid is described by the particle volume fraction, Φ_v, defined as the volume occupied by the particles per unit volume of the particle-fluid mixture. For dilute loadings ($\Phi_v < 10^{-6}$), particles act as passive tracers, and the particle-fluid interaction is described as one-way coupling. For intermediate loadings ($10^{-6} < \Phi_v < 10^{-3}$), particles do not only respond to the fluid motion but also modulate the fluid turbulence level. This type of interaction called two-way coupling is the subject of numerous previous experimental and numerical investigations aimed at quantifying the exact impact of particles on turbulence.

Tests conducted in channels (Maeda et al. 1980; Tsuji et al. 1984; Liljegren and Vlachos 1990; Kulick et al. 1994; Kiga and Pan 2002; Rani et al. 2004) and boundary layers (Rashidi et al. 1990; Best et al. 1997; Kaftori et al. 1998; Righetti and Romano 2004) by far have produced conflicting results regarding the effects of particles on the fluid mean and turbulent characteristics. Some studies indicate that the carrier fluid mean velocity is enhanced compared to the unladen flow (Maeda et al. 1980; Hagiwara et al. 2002; Righetti and Romano 2004), while others reported the mean velocity to be reduced (Best et al. 1997; Kaftori et al. 1998; Kiga and Pan 2002). Similar discrepancies exist for the carrier fluid turbulence as well. For instance, turbulence has been reported to be attenuated by small particles and augmented by large particles, with the degree of modification increasing with volume fraction (Maeda et al. 1980; Rashidi et al. 1990; Kulick et al. 1994; Pan and Banerjee 1996), whereas others (Liljegren and

Vlachos 1990; Rani et al. 2004) observed turbulence augmentation for small particles.

More often than not, particle-laden turbulent flows occur adjacent to rough surfaces, in which case, due to the presence of roughness, the flow physics can become extremely complex compared to that over a smooth wall. Roughness effects on single-phase turbulent flows are well known, which include increase in the wall shear stress, and enhancements of the turbulent intensities and Reynolds stresses by margins that may well extend into the outer flow in the case of large roughness. While particle-laden turbulence has been thoroughly characterized for smooth walls, studies over rough walls are scarce. Consequently, well-qualified rough-wall experiments are needed to provide data for comparison with current two-phase turbulence models.

In the present work, a particle image velocimetry (PIV) technique was used to perform detailed velocity measurements of a solid-liquid flow in a horizontal channel. The carrier-fluid is water. The particulate phase is glass of density 2500 kg/m^3 and mean diameter, 64 µm, carefully sieved into the size range 53 - 75 µm. The effects of particles were measured for a volumetric loading of $\Phi_v = 2 \times 10^{-4}$, which was chosen to allow two-way coupling between the phases. Clear-water and particle-laden experiments were conducted over a smooth wall and a sand grain roughness at a friction Reynolds number (Re_τ) of approximately 700. The novelty of the present work is that the statistical properties of the particles and fluid were measured for flow fields in which the particle concentration decayed over the course of the experiment due to sedimentation. This is practically relevant, for example, in the estimation of the flow fields in pneumatic conveyors, sedimentation tanks and pollutant or aerosol monitoring systems where particles may be transported without a source to maintain a constant particle volumetric flux.

EXPERIMENTAL SETUP AND METHODOLOGY

The experiments were conducted in a plane rectangular channel as shown schematically in figure 1. The channel was fabricated from 6 mm thick acrylic test plates, and has a length and internal width of 2500 mm and 186 mm, respectively. The internal height of the channel is 40 mm, which yields an aspect ratio, $b/(2h)$, of approximately 5:1, where b is the channel width and h is the channel half-height. The wall roughness, consisting of sand grains of nominal mean diameter, k = 1.5 mm ($k/h \approx 0.08$), was glued to an acrylic insert. The insert was screwed to the bottom wall of the channel to provide an asymmetric roughness in relation to the smooth upper wall. As indicated in the figure, the x coordinate is aligned with the streamwise direction, while y and z coordinates are respectively aligned with the wall-normal and spanwise directions; $x = 0$ is at the inlet of the test section and $z = 0$ is at the mid-span. The origin $y = 0$ is on the bottom wall for the smooth wall test conditions, and at the roughness crest for the rough wall test conditions.

Two trips made from a 3 mm acrylic rib were installed at the inlet of the channel, one on either wall, to quicken boundary layer transition to turbulence. The measurements were made in the mid-plane at $x/h \approx 76$ downstream of the

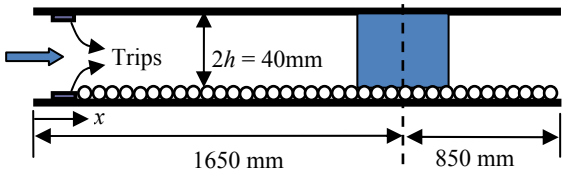

Figure 1. Schematic of the test section (not drawn to scale).

trip. The experiments were run at channel centreline velocities of approximately U_{max} = 0.75 m/s and U_{max} = 0.50 m/s, respectively, for the smooth and rough walls. The friction velocity estimated using the Clauser chart method was approximately U_τ = 0.035 m/s for the smooth and rough walls. The turbulent intensity, u/U_{max}, measured at the channel centre line was about 0.04 for the unladen smooth wall, which is in good agreement with values of 0.04 ± 10% compiled by Durst et al. (1998) for smooth pipes and channels.

In the particle-laden experiments, particles were fed into the flow at an average volume fraction of $\Phi_v = 2 \times 10^{-4}$ and were allowed to recirculate with the flow. It should be remarked that this is only a one-time loading since particles were not added to the flow on a continuous basis to maintain a steady concentration. This way, the overall particle concentration decreased over the data acquisition period due to gravitational settling. For the smooth wall, the particle Reynolds number, $Re_p = d_p|U_{rel}|/\nu$, where U_{rel} is the relative velocity between the particles and the fluid, and ν is the kinematic viscosity of the fluid, was approximately 2.0. The corresponding Stokes number, $St = \tau_p/\tau_f$, where $\tau_p = \tau_{p,Stokes}/(1 + 0.15Re_p^{0.687})$ is the corrected particle response time, $\tau_{p,Stokes} = [(2\rho_p/\rho_f + 1)d_p^2]/(36\nu)$ is the Stokesian response time, τ_f is the viscous time scale, ν/U_τ^2, and U_τ is the friction velocity, was approximately 1.0. For the rough wall, the particle Reynolds number and wall Stokes number were 13.0 and 0.5, respectively. The particle relative diameter in wall units is $d_p^+ = 2.2$.

The PIV setup consists of a 12-bit 2048 pixels × 2048 pixels CCD camera, a double-pulsed Nd-YAG laser, and a PC. The velocities of the two phases were measured separately. The velocity of the carrier fluid was detected by seeding the flow with 10 µm polymer microspheres coated in Rhodamine B. Rhodamine B is a fluorescent dye that absorbs green laser light at a wavelength of 532 nm, and fluoresces with orange light at a wavelength of 590 nm. The fluorescent light from the seeding particles was separated from the Mie scattering light due to the solid phase by equipping the camera lens with a long-pass cut-off orange filter centred on the emission wavelength of the dye. The solid phase velocity was measured using the same camera but with the orange filter replaced by a green (band-pass) filter that captured the Mie scattering light from the solid particles. Even though the green filter exposed the camera to some Mie scattered light from the fluid tracer particles, the cross talk between the two phases was very minimal due to the size difference between the particles and tracers. Data acquisition was controlled using the DynamicStudio software developed by Dantec Dynamics. For each phase an ensemble of 5000 image pairs was acquired, which is large enough for the

flow statistics to converge. The data were post-processed using the adaptive correlation option of DynamicStudio. The interrogation area (IA) size for the correlation was set to 32 pixels × 32 pixels with 50 % overlap in both x and y. The adaptive correlation algorithm used a multi-pass FFT with a one-dimensional Gaussian peak-fitting function to determine the average particle displacement within the interrogation window to sub-pixel accuracy. During the image acquisition, steps were taken to ensure that the maximum particle displacement was less than ¼ of the IA size. With an IA size of 32 pixels × 32 pixels, the maximum particle displacement in the main flow direction was 8 pixels with a dynamic range of 80. The spatial resolution and physical spacing between the velocity vectors in the y-direction were respectively 0.788 mm and 0.394 mm. In all experiments, the uncertainties in the mean velocity, turbulent intensities, and Reynolds shear stress at the 95 % confidence level were estimated as ±3 %, ±7 %, and ±10 %, respectively.

RESULTS AND DISCUSSION

Because the surface roughness was introduced onto the lower wall, the results reported here correspond to those measured in the lower half of the channel. The lower half of the channel is the flow region starting from the lower wall to the wall-normal location where the Reynolds shear stress changes sign from positive to negative. Single-point statistics presented include the mean velocity, turbulent intensities, Reynolds shear stress and quadrant decomposition of the Reynolds shear stress. All statistics were calculated by ensemble averaging and line averaging in the homogeneous streamwise direction. To facilitate the discussion, test conditions over the smooth wall and sand grain roughness are designated with acronyms SM and SG, respectively. For a given surface, the symbol Φ_o denotes measurements in clear water, while Φ_1 denotes measurements in the presence of particles.

Concentration Decay

Figure 2 shows the particle count and number density distributions of the solid phase, obtained by counting the number of particles imaged within the field of view. Figures 2a and 2b demonstrate how the total particle count per image varied over the data acquisition period. The concentration decline follows an exponential distribution. The plots in figure 2c were obtained by a least square exponential fit of the decay law $y = y_o + be^{ax}$ to the particle count data shown in figures 2a and 2b, normalized by their initial values, N_o. The values of the curve fitting parameters are summarized in Table 1. The plots show that the relative particle count, N/N_o, decays less rapidly over the rough wall than the smooth wall, the overall decay amounting to about 40% and 30% for the smooth and rough walls, respectively. These results are in qualitative agreement with LES results reported by Dritselis (2009) for a channel flow over smooth and rough walls. Figure 2d shows the particle mean number density distributions measured across the lower half of the channel, normalized by the bulk or depth-averaged number density. In the plot, the wall-normal distance, y, is normalized by the distance, h^*, which corresponds to the

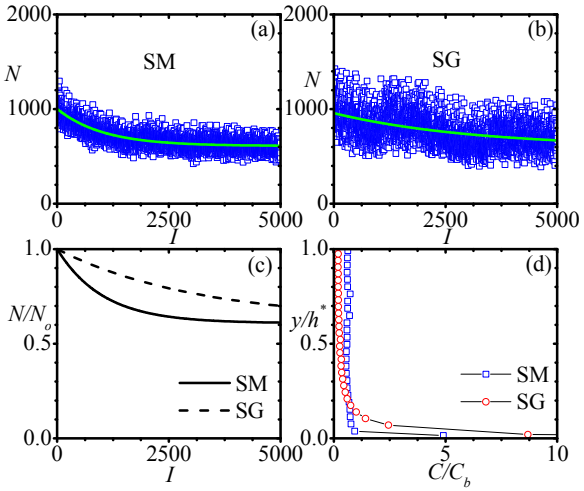

Figure 2. Particle count and number density distributions.

distance measured from the lower wall to the location of zero-crossing of the Reynolds shear stress ($-uv$). The distributions indicate that there are fewer particles in suspension away from the rough wall, but a larger number of particles close to the rough wall compared to the smooth wall. A similar observation was reported by Dritselis (2009) for the rough walls used in that study.

Table 1. Values of least square curve fitting parameters for the exponential decay law, $y = y_o + be^{ax}$.

Test	y_o	b	a	R^2
SM	610.1459	392.4344	-9.7496×10^{-4}	0.6579
SG	596.2311	361.0851	-3.1847×10^{-4}	0.2256

Distributions of the Mean Velocity and Turbulent Characteristics

Figure 3 examines the effects of particles on the carrier fluid mean velocity, turbulent intensities and Reynolds shear stress for the smooth wall and in the presence of surface roughness. The mean velocity and turbulent intensities are normalized by the maximum streamwise mean velocity U_{max}, while the Reynolds shear stress is normalized by U_{max}^2. Figure 3a shows that the mean velocity is less full in the presence of wall roughness irrespective of the loading condition when compared to the smooth wall distribution. This is consistent with observations in previous rough-wall studies that surface roughness reduces the mean velocity (Krogstad et al. 1992; Tachie et al. 2000). Over the smooth wall, the mean velocity is slightly increased for the particle-laden flow when compared to the clear water flow. This may be attributed to particles travelling faster than the fluid, dragging the flow along with them. However, this effect is overcome by the roughness so that the rough wall distributions are approximately similar for both the laden and unladen flows. The streamwise turbulent intensity (figure 3b) is enhanced (about 13%) by particles in the wall region but reduced (by about 16%) in the outer layer for the smooth wall. Over the rough wall the values are enhanced within $0.2 < y/h^* < 0.5$ by about

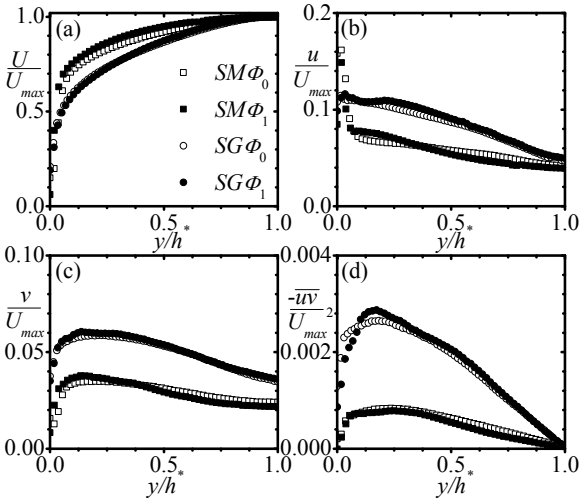

Figure 3. Distributions of the mean velocity, turbulent intensities and Reynolds shear stress for the carrier fluid.

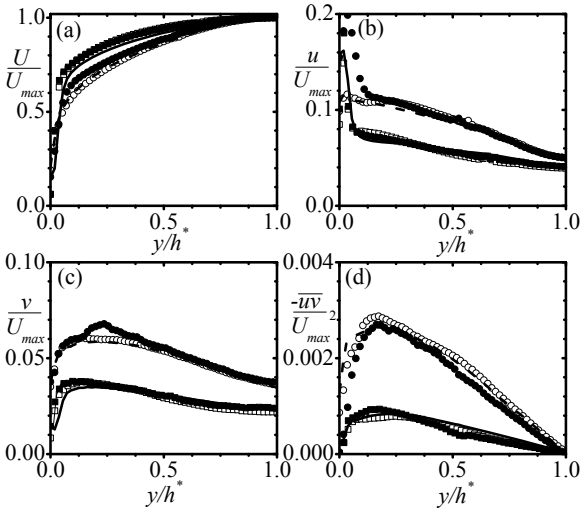

Figure 4. Distributions of the mean velocity, turbulent intensities and Reynolds shear stress compared between the carrier fluid and solid phase. Symbols: ━, $SM\Phi_0$; ╍$SG\Phi_0$; □, $SM\Phi_1$ (fluid); ■, $SM\Phi_1$ (solid); ○, $SG\Phi_1$ (fluid); ●, $SG\Phi_1$ (solid).

11% for the laden flow, but the roughness effect diminishes, leading to similarity in the profiles further out. Irrespective of the loading condition the peak streamwise turbulent intensity level is suppressed near the rough wall, although the rough wall intensity values are substantially higher than the smooth wall values for most of the flow region. The suppression in the rough wall peak values may be attributed to the disruption of the quasi-streamwise vortices by the roughness elements. Similar effects were observed in previous single-phase rough wall studies (Krogstad et al. 2005). For the wall-normal turbulent intensity (figure 3c), the presence of particles also results in enhancements near the smooth wall, but a reduction occurs in the outer region as observed for u/U_{max}. However, over the rough wall, these effects were nullified. Comparing the smooth and rough wall distributions, the levels of v/U_{max} are significantly enhanced by wall roughness over the entire flow region for both the unladen and laden flows. The effect of wall roughness is more dramatic in the Reynolds shear stress (figure 3d), and there is an additional increase of about 15% in the peak value in the presence of particles. For the smooth wall, particles produced no significant modification in the Reynolds shear stress in the wall region, but there is a reduction of up to about 28% in the outer region. These reduction reflects the trend in the outer layer values of the turbulent intensities. The increase and decrease in turbulent intensities over the present smooth wall are consistent with similar observations in previous studies (Best et al. 1997; Righetti and Romano 2004) although these studies used larger glass particles than in the present work.

Figure 4 compares the mean velocity and turbulent statistics of the solid phase to corresponding distributions for the clear and particle-laden fluids. For the smooth wall, the solid mean velocity matches that of the laden fluid, but exceeds that of the clear water by up to about 8% in the inner half of the flow region. Surface roughness flattens the solid mean velocity profile resulting in larger values than the corresponding clear and laden fluid values in the inner region. The solid streamwise velocity fluctuation intensity matches the unladen fluid distribution for the smooth wall, but the peak value is dramatically increased in the presence of the rough wall; in the outer parts of the rough wall flow, solid and carrier fluid distributions are similar. The solid wall-normal velocity fluctuation intensity for the smooth wall is similar to that of the laden flow. The peak value for the rough wall, on other hand, is about 15% larger than the corresponding unladen fluid value. In the outer layer, no significant differences are observed. The larger values of the rough wall peak particle velocity fluctuation intensities may be partly attributed to particle-wall collisions, which as have been noticed in previous studies (Benson et al. 2005; Lain and Sommerfeld 2008), significantly increase the velocity fluctuations near a rough wall. For the solid Reynolds shear stress, the peak value over the smooth wall is about 28% higher than the unladen fluid peak value, but there is a reduction of up to about 30% in the values in the outer layer. Over the rough wall, solid and unladen fluid Reynolds shear stress distributions reached similar peaks, but differences are observed elsewhere across the flow region. The laden fluid Reynolds shear stress exceeds that of the solid phase for nearly the entire flow region due to larger values of the Reynolds shear stress correlation coefficient in the laden fluid (not shown).

Quadrant Decomposition

Quadrant decomposition is a useful tool for examining the Reynolds shear stress producing events in turbulence. With this technique the instantaneous Reynolds shear stress u_iv_i is sorted into the four quadrants of the u-v plane: Q1 (outward interactions) when both u_i and v_i are positive, Q2 (ejections) when u_i is negative and v_i is positive, Q3 (inward interactions) when both u_i and v_i are negative, and Q4 (sweeps) when u_i is positive and v_i is negative. The inward and outward interaction terms contribute only positive Reynolds shear stress, while ejections and sweeps contribute negative Reynolds shear stress. Ejections

transport low-momentum fluid away from the wall to the outer layer, while sweeps transport high-momentum fluid from the outer layer to the wall region. Following the methodology proposed by Lu and Willmarth (1973), the mean Reynolds shear stress at a given wall-normal location is decomposed into contributions from the four quadrants Q1, Q2, Q3 and Q4 excluding a hyperbolic hole of size H as

$$\langle uv\rangle_Q(x,y,H)=\frac{1}{N}\sum_{i=1}^{N}u_i(x,y)v_i(x,y)S_Q(x,y,H) \quad (1)$$

where N is the total number of instantaneous velocity vectors (= total number of PIV snapshots) at a given wall-normal location and S_Q is a detector function given by

$$S_Q(x,y,H)=\begin{cases}1, \text{ when } |u_i(x,y)v_i(x,y)|_Q \geq Hu_{rms}(x,y)v_{rms}(x,y)\\ 0, \text{ otherwise}\end{cases} \quad (2)$$

Figure 5 presents the quadrant decomposition results for the carrier fluid obtained with hyperbolic hole size $H = 2$. This value of H is used to ensure that only strong events are considered in the decomposition, and represents instantaneous Reynolds shear stress values larger than about 5 times the mean Reynolds shear stress. The contributions for the unladen flow are in good agreement with those presented by Krogstad et al. (2005) for a turbulent channel experiment and DNS. The quadrant decomposition shows that the outward and inward interaction terms (figures 5a and 5b) are unimportant except in the core region. The more dominant contributors to the Reynolds shear stress, ejections and sweeps, are shown in figures 5c and 5d, respectively. Particles increased ejections in the outer layer for the smooth wall, but produce no significant effect over the rough wall. Another interpretation is that the increase in ejections by particles that is observed for the smooth wall, is offset by attenuation of these events when the laden flow encounters wall roughness. Sweeps are independent of the surface condition and particles in the near wall region, but are attenuated by the particles in the region $0.12 < y/h^* < 0.7$ for the smooth wall case. No significant effects are observed in the sweeps when the laden flow is subjected to wall roughness, except in the core region. However, differences in the core region are of no consequence since the Reynolds shear stress is small in the core region (zero at the centreline). Figures 5e and 5f show the proportion of ejections and sweeps residing in the second and fourth quadrants, respectively. The values of N_{Q2} can be used as a rough measure of the bursting frequency in the flow. Figure 5e shows that surface roughness enhanced the bursting frequency both for the clear water and in the presence of particles. For the smooth wall, loading the flow with particles reduces the bursting frequency near the wall, increases it away from the wall, but there is a further reduction near the core region. For the rough wall, the effect of loading is only important over a limited region in the outer layer where an increase is observed. The proportion of sweeps (figure 5f) is also enhanced by roughness in the inner region for both the laden and unladen flow, but the effect extends much further into the outer layer for the laden flow than for the unladen flow.

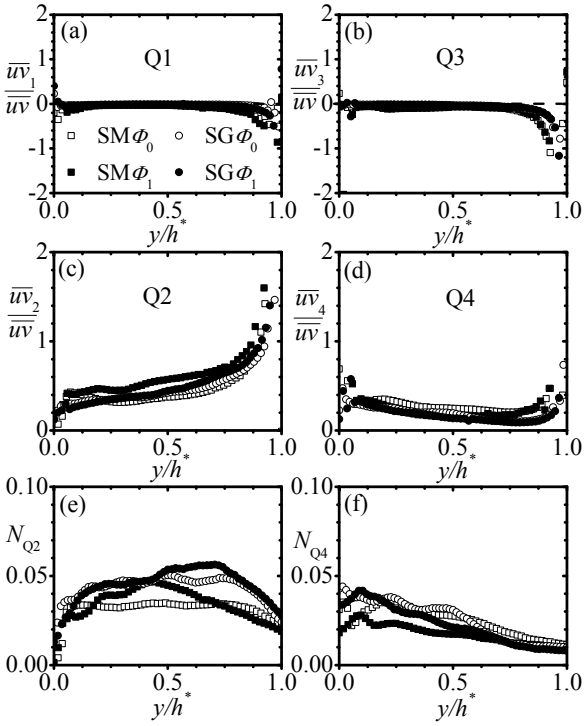

Figure 5. Quadrant decomposition of the carrier fluid Reynolds shear stress.

Maintaining the surface condition and loading the flow with particles generally reduces the number of sweeps. The effect is larger over the rough wall than observed for the smooth wall. When the particle-laden flow is subjected to wall roughness, the proportions of the ejections and sweeps were increased in regions where they were reduced by the particles for the smooth wall case. Thus, the overall effect on the Reynolds shear stress would be a balance between these opposing influences of roughness and particles.

SUMMARY AND CONCLUSIONS

A particle image velocimetry technique was employed to characterize particle-turbulence interactions in the presence of a rough wall. The tests were conducted in a horizontal channel in which the carrier fluid, which is water, was laden with small ($d_p^+ = 2.2$) glass particles at an average volume fraction of 2×10^{-4}. The solid particles recirculated with the flow, but their concentration was allowed to decay over the course of the experiments by sedimentation. It was found that for the smooth wall, particles increased the streamwise and wall-normal turbulent intensities in the wall region, and reduced them in the outer layer. These effects are less important for the rough wall. However, wall roughness reduced the peak values of the streamwise turbulent intensity for the laden and unladen flows in comparison with the smooth wall values due to the disruption of the near wall vortical structures. Over most of the outer region, the streamwise turbulent intensity is substantially increased for the rough wall cases in comparison with the smooth wall irrespective of loading. Strong enhancements were also

observed in the wall-normal turbulent intensity for the entire flow region, but the most dramatic increase with roughness occurred in the Reynolds shear stress, where the peak value was increased by more than three-fold, accompanied by a further enhancement in the presence of particles. The particulate phase measurements show that roughness reduces the solid phase streamwise mean velocity in comparison with the smooth wall values just as it reduces that of the unladen fluid, but the effect is smaller for the solid phase than the unladen fluid. The present results show that the settling particles travel appreciably faster than the carrier fluid for the rough wall case. For the rough wall, the peak values of the particle velocity fluctuation intensities exceed those of the unladen and particle-laden flows due to more frequent particle-wall collisions, but the effect is stronger for the streamwise velocity fluctuation intensity. In spite of the larger peak velocity fluctuation intensities for the rough wall, the corresponding particle Reynolds shear stress is smaller compared to the unladen fluid due to reduced correlation between the velocity fluctuation intensities. Overall, these results indicate that the particle motion is more responsive to the presence of the rough wall than the carrier fluid due to particle-wall collisions.

REFERENCES

Best, J., Bennet, S., Bridge, J. and Leeder, M., 1997, "Turbulence Modulation and Particle Velocities over Flat sand Beds at Low Transport Rates," *Journal of Hydraulic Engineering*, Vol. 123(12), pp. 1118-1129.

Benson, M., Tanaka, T., and Eaton, J.K., 2005, "Effects of Wall Roughness on Particle Velocities in a Turbulent Channel Flow," Journal of Fluids Engineering, Vol. 127, pp. 250-256.

Dritselis, C.D., 2009, "LES of Particle-Laden Turbulent Channel Flow with Transverse Roughness Elements on One Wall," *Numerical Analysis and Applied Mathematics*, Vol. 2, pp. 677-680.

Durst, F., Fischer, M., Jovanovic, J., and Kikura, H., 1998, "Methods to Set Up and Investigate Low Reynolds Number, Fully Developed Turbulent Plane Channel Flows," *Journal of Fluids Engineering*, Vol. 120(3), pp. 496-503.

Hagiwara, Y., Murata, T., Tanaka, M., and Fukawa, T., 2002, "Turbulence Modification by the Clusters of Settling Particles in Turbulent Water Flow in a Horizontal Duct," *Powder Technology*, Vol. 125, pp. 158-167.

Kaftori, D., Hetsroni, G. and Banerjee, S., 1998, "Effects of Particles on Wall Turbulence," *International Journal of Multiphase Flow*, Vol. 24(3), pp. 359-386.

Kiga, K.T. and Pan, C., 2002, "Suspension and Turbulence Modification Effects of Solid Particulates on a Horizontal Turbulent Channel Flow," *Journal of Turbulence*, Vol. 3, pp. 1-21.

Krogstad, P. -Å., Andersson, H.I., Bakken, O.M. and Ashrafian, A., 2005, "An Experimental and Numerical Study of Channel Flow with Rough Walls," *Journal of Fluid Mechanics*, Vol. 530, pp. 327-352.

Krogstad, P. -Å., Antonia, R.A. and Browne, L.W.B., 1992, "Comparison between Rough-and Smooth-Wall Turbulent Boundary Layers," *Journal of Fluid Mechanics*, Vol. 245, pp. 599-617.

Kulick, J.D., Fessler, J.R. and Eaton, J.K., 1994, "Particle Response and Turbulence Modification in Fully Developed Channel Flow," *Journal of Fluid Mechanics*, Vol. 277, pp. 109-134.

Lain, S., and Sommerfeld, M., 2008, "Euler/Lagrange Computations of Pneumatic Conveying in a Horizontal Channel with Different Wall Roughness," *Powder Technology*, Vol. 184, pp. 76-88.

Liljegren, L.M., and Vlachos, N.S., 1990, "Laser Velocimetry Measurements in a Horizontal Gas-Solid Pipe Flow," *Experiments in Fluids*, Vol. 9, pp. 205-212.

Lu, S. S., and Willmarth, W. W. 1973, "Measurements of the Structure of the Reynolds Stress in a Turbulent Boundary Layer," *Journal of Fluid Mechanics*, Vol. 60, pp. 481-512.

Maeda, M., Hishida, K. and Furutani T., 1980, "Optical Measurements of Local Gas and Particle Velocity in an Upward Flowing Dilute Gas-Solids Suspension," *Proceedings of Polyphase Flow and Transport Technology*, Century 2-ETC, San Francisco, pp. 211-216.

Pan, Y., and Banerjee, S., 1996, "Numerical Simulation of Particle Interactions with Wall Turbulence," *Physics of Fluids*, Vol. 8 (10), pp. 2733-2755.

Rani, S.L., Winkler, C.M., and Vanka, S.P., 2004, "Numerical Simulations of Turbulence Modulation by Dense Particles in a Fully Developed Pipe Flow," *Powder Technology*, Vol. 141, pp. 80-99.

Rashidi, M., Hetsroni, G. and Banerjee, S., 1990, "Particle-Turbulence Interaction in a Boundary-Layer," *International Journal of Multiphase Flow*, Vol. 16, pp. 935-949.

Righetti, M. and Romano, G.P., 2004, "Particle-Fluid Interactions in a Plane Near-Wall Turbulent Flow," *Journal of Fluid Mechanics*, Vol. 505, pp. 93-121.

Tachie, M.F., Bergstrom, D.J. and Balachandar, R., 2000, "Rough-Wall Turbulent Boundary Layers in Shallow Open Channel Flow," *Journal of Fluids Engineering*, Vol. 122, pp. 533-541.

Tsuji, Y., Morikawa, Y. and Shiomi, H., 1984, "LDV Measurements of an Air-Solid Two-Phase Flow in a Vertical Pipe," *Journal of Fluid Mechanics*, Vol. 139, pp. 417-434.